

Fermi Momentum Corrections in Deuterium

E.S. SMITH

1 Introduction

We have been studying the production of baryonic states using deuterium as a neutron target. When the final state contains a missing neutral (e.g. a neutron), missing-mass techniques are limited by the Fermi motion of the target neutron. In this note we investigate methods to minimize the effects of this smearing, i.e. ways to improve the resolution of measured quantities by appropriate analysis techniques. We use the production of the $\Lambda^*(1520)$ off the proton in deuterium to test various correction schemes:

$$\begin{aligned} \gamma p &\rightarrow K^+ \Lambda^*(1520) \\ &\hookrightarrow K^- p \end{aligned} \tag{1}$$

This reaction has the same kinematics as reactions on the neutron, but can be completely overdetermined by measuring all particles in the final state. We assume that procedures which are successful in the reconstruction of this reaction, while ignoring the possibly known momentum of the proton, can be used for the reconstruction of other reactions with an undetected neutron.

We first introduce some notation for the sum of the beam and target four vectors:

$$P = p_\gamma + p_T \tag{2}$$

$$M_\Lambda^2 = (P - p_{K^+})^2 \tag{3}$$

$$M_N^2 = (P - p_{K^+} - p_{K^-})^2 \tag{4}$$

The goal of this study is to consider the resolution of the measurement of M_Λ^2 when the proton is undetected. In this case, the Fermi momentum in the target limits the measurement of this quantity using the missing-mass technique as shown in Fig. 1, and no peak is visible in the spectrum. We investigate how to determine the quantity $M_\Lambda^2(0)$ in the absence of Fermi smearing by using constraints between measured quantities in the reaction. In this note we compare three different methods for improving the resolution.

2 Data sample

The data sample includes skimmed files from the entire g2 photon run period. The skimming process was accomplished in two steps. The first skim was part of the standard cooking for the g2 data and selected all events with positive tracks in the final state with a part-bank mass between 0.3 and 0.7 GeV. The data set was further reduced in a second step that required a negative track in every event. When this second skim was produced, “bad” files were eliminated and files from one run were consolidated into a single file. The resulting data sample consists of 231 files on the g2 cache disk and correspond to runs between 20020 and 20698. Runs 20020–20352 were taken at an electron beam energy of 2.478 GeV and runs 200584–20698 were taken with an electron beam energy of 3.115 GeV [1]. In order to enhance the photon flux at higher energy, the runs were triggered with limited ranges of T-counters. The skimmed data set, which requires two kaons, also has a selection bias for the higher energy photons.

3 Empirical Corrections

The SPring-8 collaboration has adopted an empirical approach to corrections to the reconstructed missing mass, which have been shown to work for the case of Σ^+ production [2]. Their corrected missing mass is given by:

$$M_\Lambda(0) \simeq M_\Lambda - f(M_N - m_N), \quad (5)$$

where the correction parameter f is equal to 1, and m_N is the nucleon mass. The motivation for such approach is described in an informal note by Ken Hicks [3], where he determines that the factor $f = 0.8$ is a better value for the CLAS g2 data set which we use subsequently in this analysis. We take Eq. 5 as the defining equation for the missing mass correction and investigate various ways of determining f , which might vary depending of the kinematics of the event.

4 Nucleon mass as a constraint

When a particle is missing, a powerful constraint results by using the known mass of the assumed missing particle. For example, if the reaction is assumed to take place on a proton (or neutron) and this is the undetected particle, then the missing four-momenta can be reconstructed using the measured missing momenta and the known nucleon mass:

$$\vec{p}_{miss} = \vec{P} - \vec{p}_{K^+} - \vec{p}_{K^-} \quad (6)$$

$$p_{miss} = (E, \vec{p}_{miss}) \quad (7)$$

$$E = \sqrt{\vec{p}_{miss}^2 + m_N^2} \quad (8)$$

The substitution of E in Eq. 8 for the energy of the “missing” proton in Eq. 1 can result in considerable improvement in the reconstruction of the kinematics of the event. This is especially true in the case where the energies are dominated by the masses of particles and uncertainties in the determination of the missing three-momenta contribute relatively little to reconstructed missing mass. The four-vector of the missing particle determined in this way can then be used to construct “invariant mass” quantities, such as that of the $\Lambda^*(1520)$:

$$M_\Lambda(0) \simeq \sqrt{(p_{miss} + p_{K^-})^2}$$

$$f = \frac{M_\Lambda - \sqrt{(p_{miss} + p_{K^-})^2}}{M_N + m_N}. \quad (9)$$

5 Kinematical corrections

Using standard notation for many variables, we can compute the kinematical variables of interest assuming that the target proton in Deuterium has Fermi momentum p_F which is small relative to its mass M_T .

$$p_T = \left(M_T + \frac{p_F^2}{2M_T}, \vec{p}_F \right). \quad (10)$$

Each kinematic variable is considered a function of the Fermi momentum and reduces to the case of scattering off a stationary target when p_F is zero.

$$s = P^2 \quad (11)$$

$$s = 2E_\gamma \left(M_T + \frac{p_F^2}{2M_T} - p_F \cos \theta_F \right) + M_T^2 \quad (12)$$

$$s(p_F^2 = 0) = 2E_\gamma M_T + M_T^2 \quad (13)$$

$$s - s(0) = E_\gamma \frac{p_F^2}{M_T} - 2\vec{p}_\gamma \cdot \vec{p}_F \quad (14)$$

The mass of the $\Lambda^*(1520)$, in “missing mass,” can be computed using momentum and energy conservation

$$M_\Lambda^2 = (P - p_{K^+})^2 \quad (15)$$

$$M_\Lambda^2 = s - 2E_{K^+} \left(E_\gamma + M_T + \frac{p_F^2}{2M_T} \right) + 2E_\gamma p_{K^+}^z + 2\vec{p}_F \cdot \vec{p}_{K^+} + M_K^2 \quad (16)$$

$$M_\Lambda^2(0) = s(0) - 2E_{K^+}(E_\gamma + M_T) + 2E_\gamma p_{K^+}^z + M_K^2 \quad (17)$$

$$M_\Lambda^2 = M_\Lambda^2(0) + (E_\gamma - E_{K^+}) \frac{p_F^2}{M_T} + 2\vec{p}_F \cdot (\vec{p}_{K^+} - \vec{p}_\gamma) \quad (18)$$

$$M_\Lambda^2 \simeq M_\Lambda^2(0) + 2\vec{p}_F \cdot (\vec{p}_{K^+} - \vec{p}_\gamma) \quad (19)$$

$$\equiv M_N^2(0) + 2|p_F| \cdot |\vec{p}_{K^+} - \vec{p}_\gamma| \cdot \cos \theta_{K^+-\gamma} \quad (20)$$

In the last step we have neglected the quadratic term in p_F compared to the linear term. In a similar way one can compute the mass of the missing nucleon using

$$M_N^2 = (P - p_{K^+} - p_{K^-})^2 \equiv (P - p_{KK})^2 \quad (21)$$

$$M_N^2 = s - 2E_{KK} \left(E_\gamma + M_T + \frac{p_F^2}{2M_T} \right) + 2E_\gamma p_{KK}^z + 2\vec{p}_F \cdot \vec{p}_{KK} + M_{KK}^2 \quad (22)$$

$$M_N^2(0) = s(0) - 2E_{KK}(E_\gamma + M_T) + 2E_\gamma p_{KK}^z + M_{KK}^2 \quad (23)$$

$$M_N^2 = M_N^2(0) + (E_\gamma - E_{KK}) \frac{p_F^2}{M_T} + 2\vec{p}_F \cdot (\vec{p}_{KK} - \vec{p}_\gamma) \quad (24)$$

$$M_N^2 \simeq M_N^2(0) + 2|p_F| \cdot |\vec{p}_{K^+} - \vec{p}_\gamma| \cdot \cos \theta_{KK-\gamma} \quad (25)$$

We have used the abbreviated notation of ‘‘KK’’ for the sum of positive and negative kaon momenta and energies. In the absence of Fermi smearing, $M_N(0)$ should equal the nucleon mass $m_N = 0.94$ GeV. Combining Eq. 25 and Eq. 20 we obtain the following relation:

$$\frac{M_\Lambda^2 - M_\Lambda^2(0)}{M_N^2 - m_N^2} = \frac{|\vec{p}_{K^+} - \vec{p}_\gamma|}{|\vec{p}_{KK} - \vec{p}_\gamma|} \left(\frac{\cos \theta_{K^+-\gamma}}{\cos \theta_{KK-\gamma}} \right) \quad (26)$$

With the approximation that

$$M_\Lambda^2 - M_\Lambda^2(0) \simeq 2M_\Lambda (M_\Lambda - M_\Lambda(0)), \quad (27)$$

We obtain the following equation:

$$M_\Lambda(0) \simeq M_\Lambda - \frac{|\vec{p}_{K^+} - \vec{p}_\gamma|}{|\vec{p}_{KK} - \vec{p}_\gamma|} \left(\frac{\cos \theta_{K^+-\gamma}}{\cos \theta_{KK-\gamma}} \right) \left(\frac{M_N + m_N}{2M_\Lambda} \right) (M_N - m_N). \quad (28)$$

Unfortunately, we do not have enough information to determine both p_F and the relative angles. However, the ratio of the cosine of the angles relative to the Fermi momentum vector should be close to unity if the angle between the two vectors is small. In addition, due to the random nature of the Fermi motion, we can expect that the ratio will be unity on average as well. In the limit in which the photon momentum

is large compared to the kaon momenta, this will be a good approximation. Making the assumption that

$$\left(\frac{\cos \theta_{K^+ - \gamma}}{\cos \theta_{K^- - \gamma}} \right) \simeq 1, \quad (29)$$

then we obtain the following formula for a correction for the Fermi momentum

$$M_\Lambda(0) \simeq M_\Lambda - \frac{|\vec{p}_{K^+} - \vec{p}_\gamma|}{|\vec{p}_{K^-} - \vec{p}_\gamma|} \left(\frac{M_N + m_N}{2M_\Lambda} \right) (M_N - m_N) \quad (30)$$

We see that this scheme is very similar to Eq. 5 where the constant factor $f = 0.8$ is replaced by an expression which depends on kinematics. To estimate the reliability of this approximation, we can employ the tracks in our event sample and determine their angles relative to a randomly generated Fermi momentum vector. These distributions are shown in Fig. 2. The top figures in the figure correspond to $\cos \theta_{K^+ - \gamma}$ and $\cos \theta_{K^- - \gamma}$ relative to an isotropically generated Fermi momentum vector for each event. The ratio in Eq. 29 is plotted in the bottom figures for the case of K^+ and K^- production which correspond to scattering off proton and neutron targets. Differences indicate small kinematic differences for each case. The correction factor in Eq. 30 is plotted in Fig. 3 for the cases of K^+ and K^- .

6 Kinematically complete events

For events where the K^+ , K^- , and the proton are all detected, the mass of the $\Lambda^*(1520)$ can be determined directly from the invariant mass of the proton and the K^- . This determination is not affected by the Fermi momentum in the target, so can be used to determine the “correct” value of the correction factor f ¹:

$$\begin{aligned} M_\Lambda(0) &\simeq \sqrt{(p_p + p_{K^-})^2} \\ f &= \frac{M_\Lambda - \sqrt{(p_p + p_{K^-})^2}}{M_N + m_N}. \end{aligned} \quad (31)$$

For this sample of events, this value can be used to check the accuracy of the other approximations.

7 Discussion

The empirical correction scheme in Eq. 5 is seen to work in calibration reactions, so the kinematical corrections of Eq. 30 must be close to the value of 0.8 if they are to

¹The proton energy has not been corrected for energy loss, so improved resolution may be possible

provide useful corrections to the data. For the g2 data set, the correction factor in Eq. 30 is plotted in Fig. 3, top left for the K^+ missing mass and top right for the K^- missing mass cases. For the case of the K^+ missing mass, which is to be compared to the empirical correction above, we see that the average correction factor is 0.82 compared to 0.8. We note that the distribution for the correction to the K^- missing mass is actually slightly broader and has an average value of 0.96. This is due to the differences in kinematics between K^+ and K^- in our data sample. In the bottom of the figure we plot the correction factors determined using Eq. 9 and Eq. 31. The correction factor as determined from the kinematically complete events is broader than the other estimates, but peaks in approximately the same place with an average value of 1. The differences of the correction factors relative to this one are shown in Fig. 4. The corrections using the nucleon mass as a constraint (Eq. 30) has the smallest rms, indicating a slight preference for this method (rms=0.72 compared to 0.75 for the other two methods).

In Fig. 5 we show the corrected missing mass distributions using the three correction methods developed here. Also indicated are the number of fitted Λ^* 's from each of the corrected distribution. Eqs. 30 and 9 determine the number of Λ^* 's to be approximately 100, compared to the number obtained from Eq. 5 which gives a value of 88. The numbers are in fact consistent within the errors of the fit. However, the larger number of fitted Λ^* 's probably indicates that the resolution function is slightly better for the kinematic corrections compared to the constant correction of Eq. 5. A direct comparisons of the distributions is shown as an overlay in Fig. 6.

8 Conclusion

All three corrections considered here improve the missing mass resolution of reaction 1. There are slight indications that Eq. 9 is the best procedure based on the comparison with the correction factor determined from kinematically complete events. In addition, this procedure is recommended mainly because it simply constrains the mass of the missing particle to have the nucleon mass, and is therefore the easiest to understand.

References

- [1] <http://www.jlab.org/~clasg2>.
- [2] T. Nakano et.al., "Observation of S=+1 Baryon Resonance in Photoproduction from Neutron," hep-ex/0301020.

[3] K. Hicks, “Unknown energy correction,” private communication, Oct 2002.

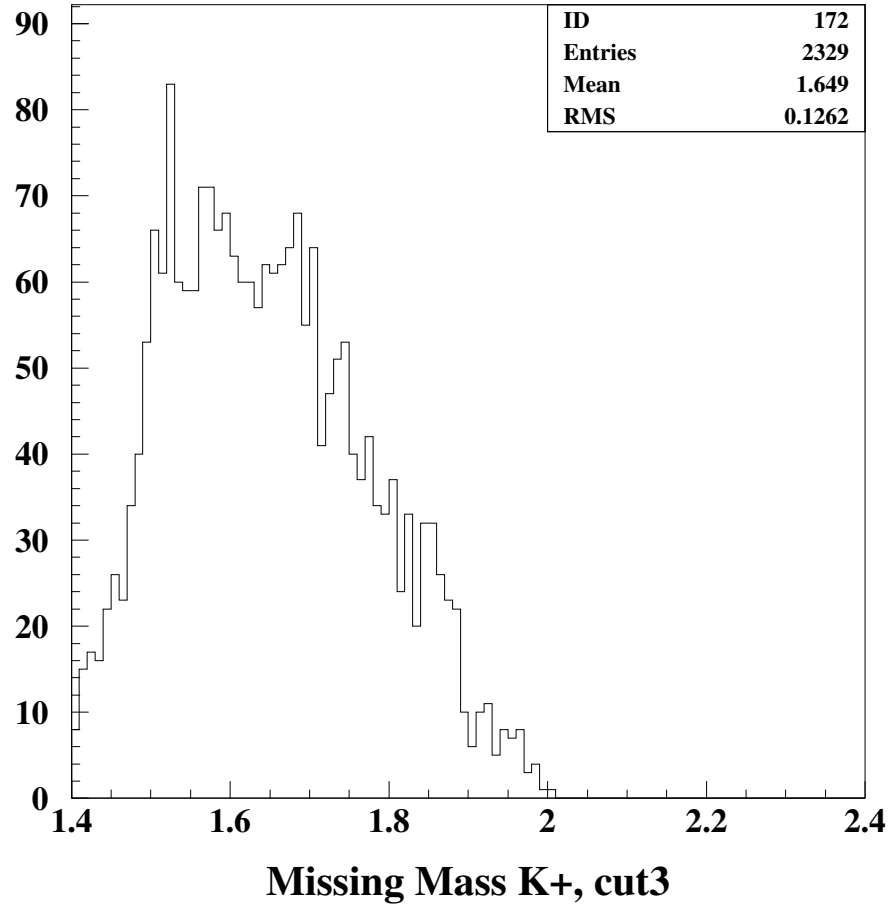


Figure 1: The missing mass corresponding to the $\Lambda^*(1520)$ computed for the reaction $\gamma p \rightarrow K^+ X$ assuming the target proton is at rest. No peak is visible in this uncorrected spectrum.

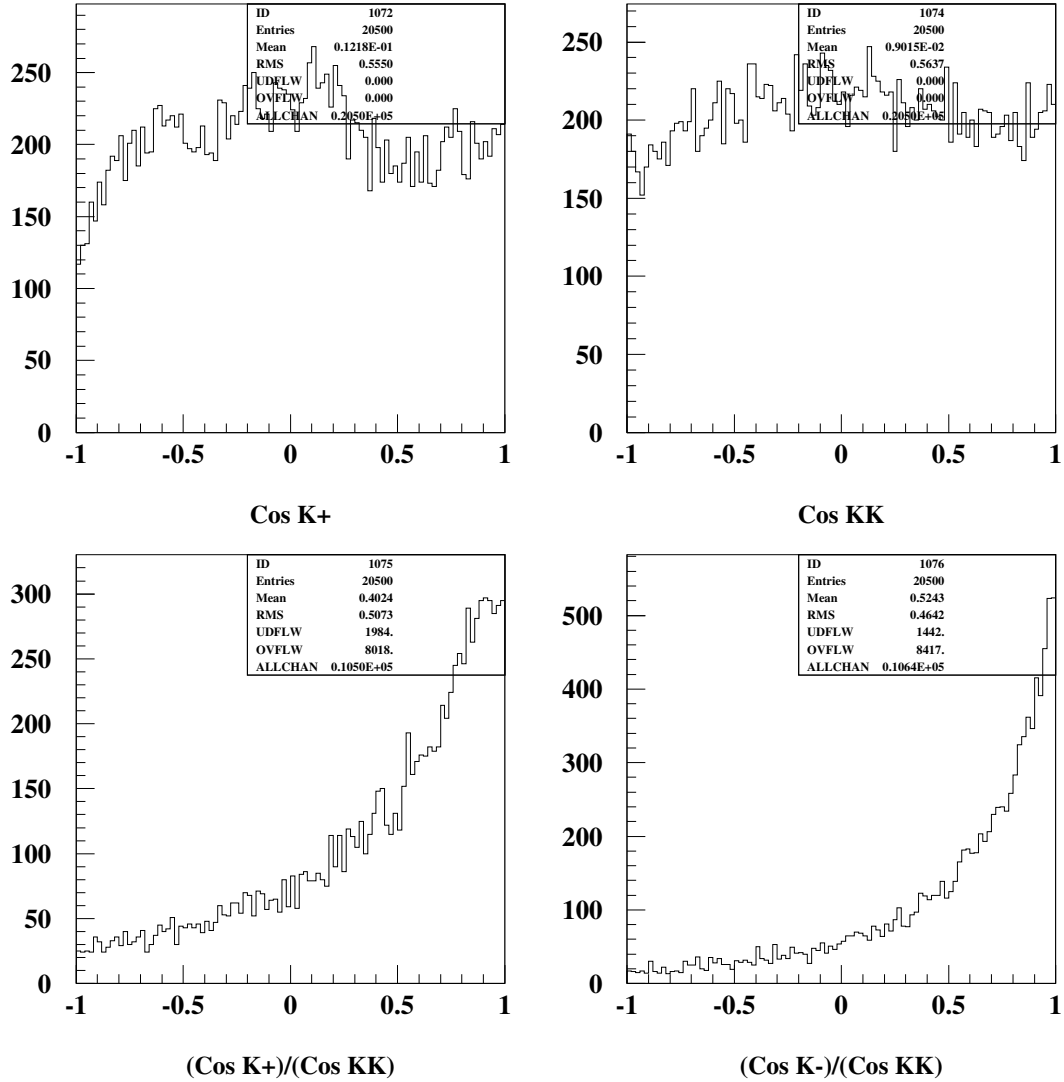


Figure 2: Distribution of the cosine ratios in Eq.29 are estimated from the data assuming that the angle of the Fermi momentum is isotropic. The Fermi direction is generated randomly and then the angle is computed between the measured kaon vectors and this randomly generated vector (Top figures). The bottom figures are the distributions for the ratio in Eq.29 for the case of scattering off the proton (left) and for the case of scattering off the neutron (right). The approximation in Eq.30 assumes that these ratios are unity.

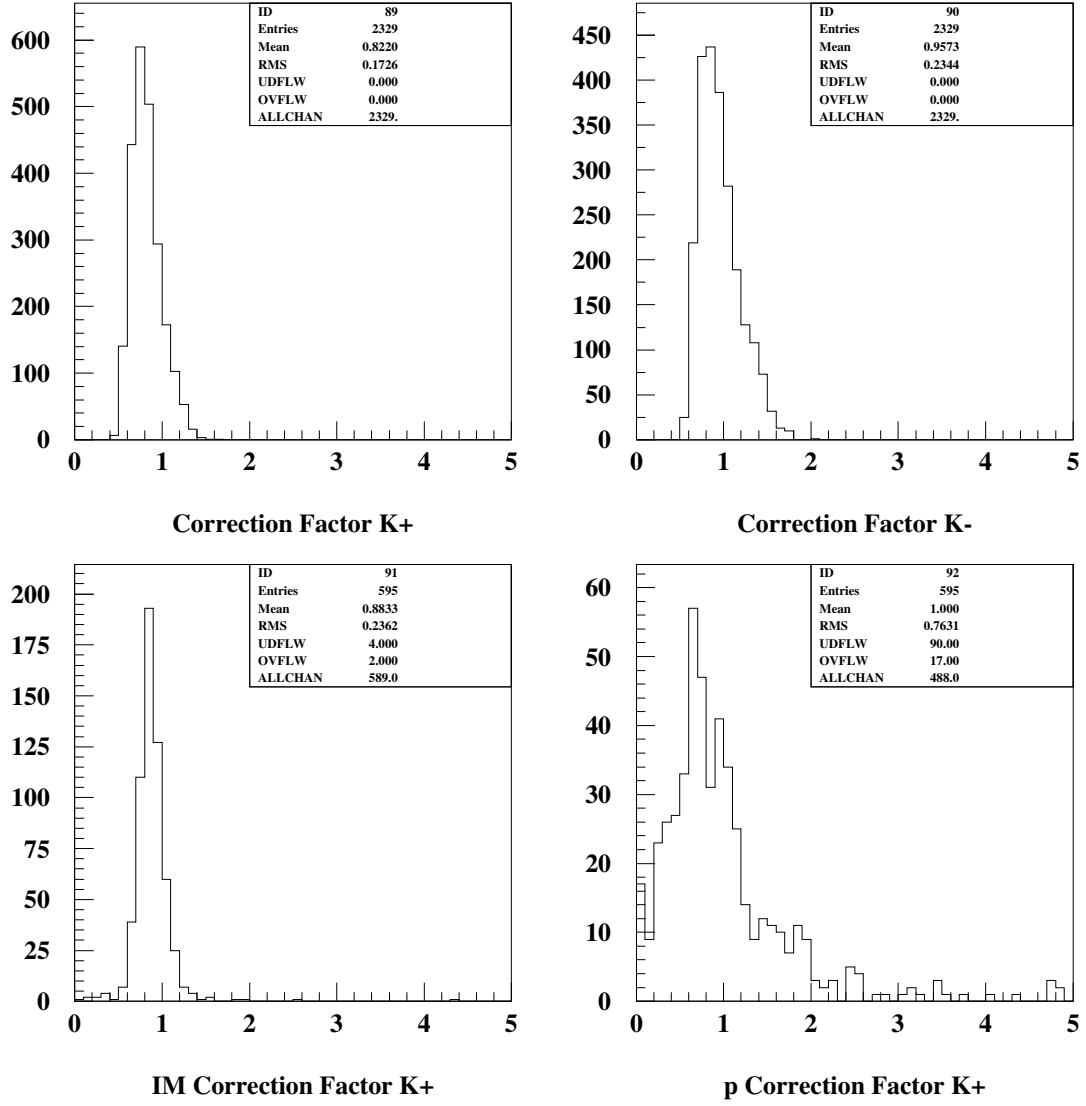
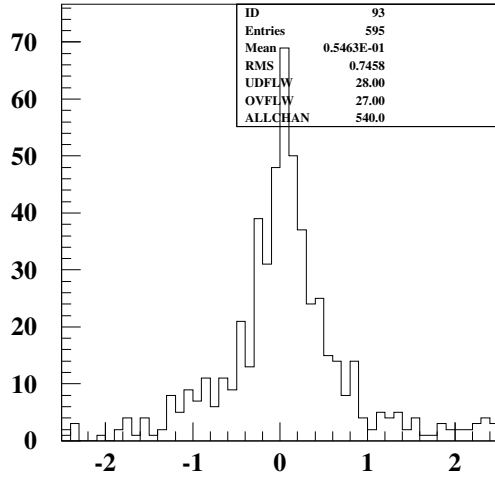
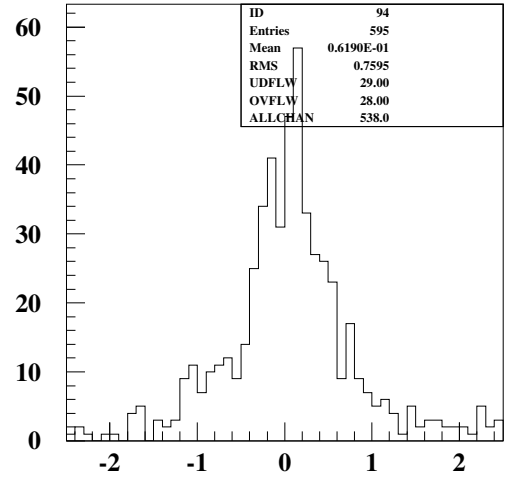


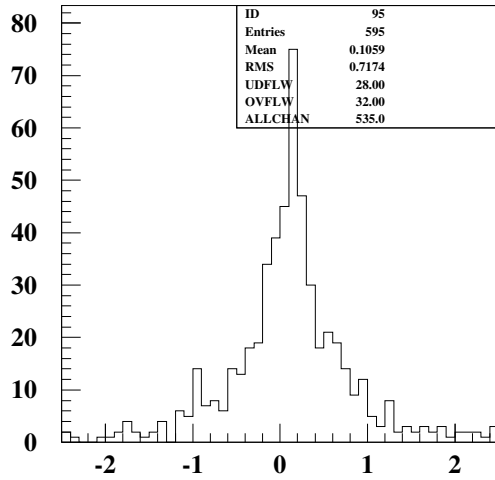
Figure 3: (Top Left) Correction factor for K^+ missing mass using Eq. 30. (Top right) Correction factor for K^- missing mass using Eq. 30. (Bottom left) Correction factor for K^+ missing mass using Eq. 9. (Bottom right) Correction factor using Eq. 31 and the K^- -p invariant mass for events with a reconstructed proton.



Correction Factor K+, Eq-p

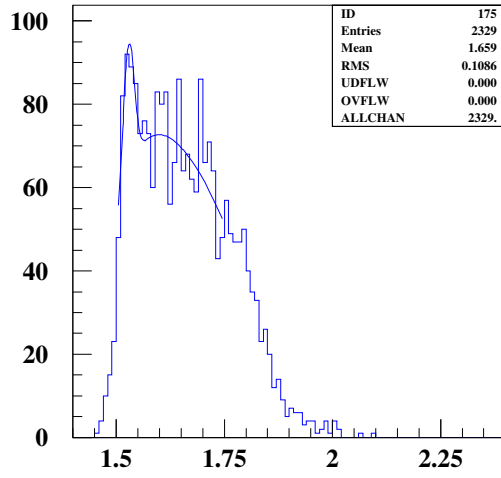


Correction Factor K+, 0.8-p

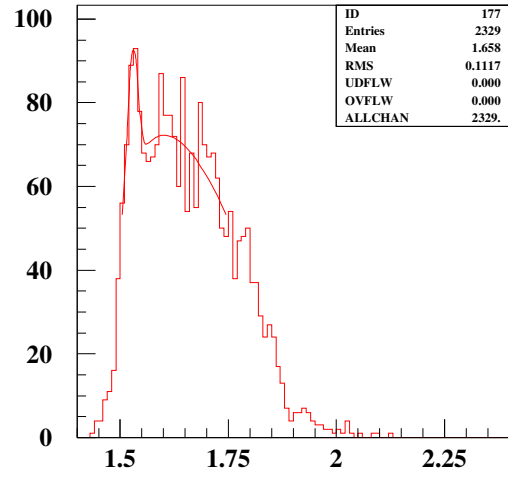


Correction Factor K+, IM-p

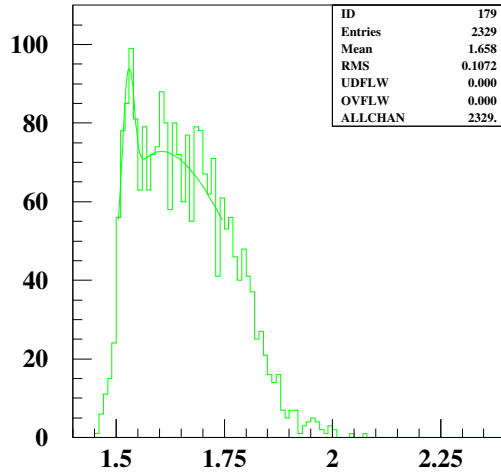
Figure 4: Differences between the K^+ missing mass correction factors and the correction factor as determined by kinematically complete events (Eq. 31). Corrections factors were computed using Eq. 30 (Top left) Eq. 5 (Top right) and Eq. 9 (Bottom left).



Mass plambda, cut3



Mass plambda, cut3, 0.8



Mass plambda, cut3, eq

IM

$$N_{\Lambda} = 99.9286 \pm 36.7946$$

$$M_{\Lambda} = 1.52893 \text{ GeV } \sigma = 12.391 \text{ MeV}$$

MM 0.8

$$N_{\Lambda} = 87.8242 \pm 36.1471$$

$$M_{\Lambda} = 1.52895 \text{ GeV } \sigma = 11.168 \text{ MeV}$$

MM Eq

$$N_{\Lambda} = 100.675 \pm 35.4915$$

$$M_{\Lambda} = 1.52837 \text{ GeV } \sigma = 12.3998 \text{ MeV}$$

Figure 5: (Top left, “IM”) Corrected distribution using Eq. 9. (Top right, “MM 0.8”) Corrected distribution using Eq. 5. (Bottom, “MM Eq”) Corrected distribution using Eq. 30.

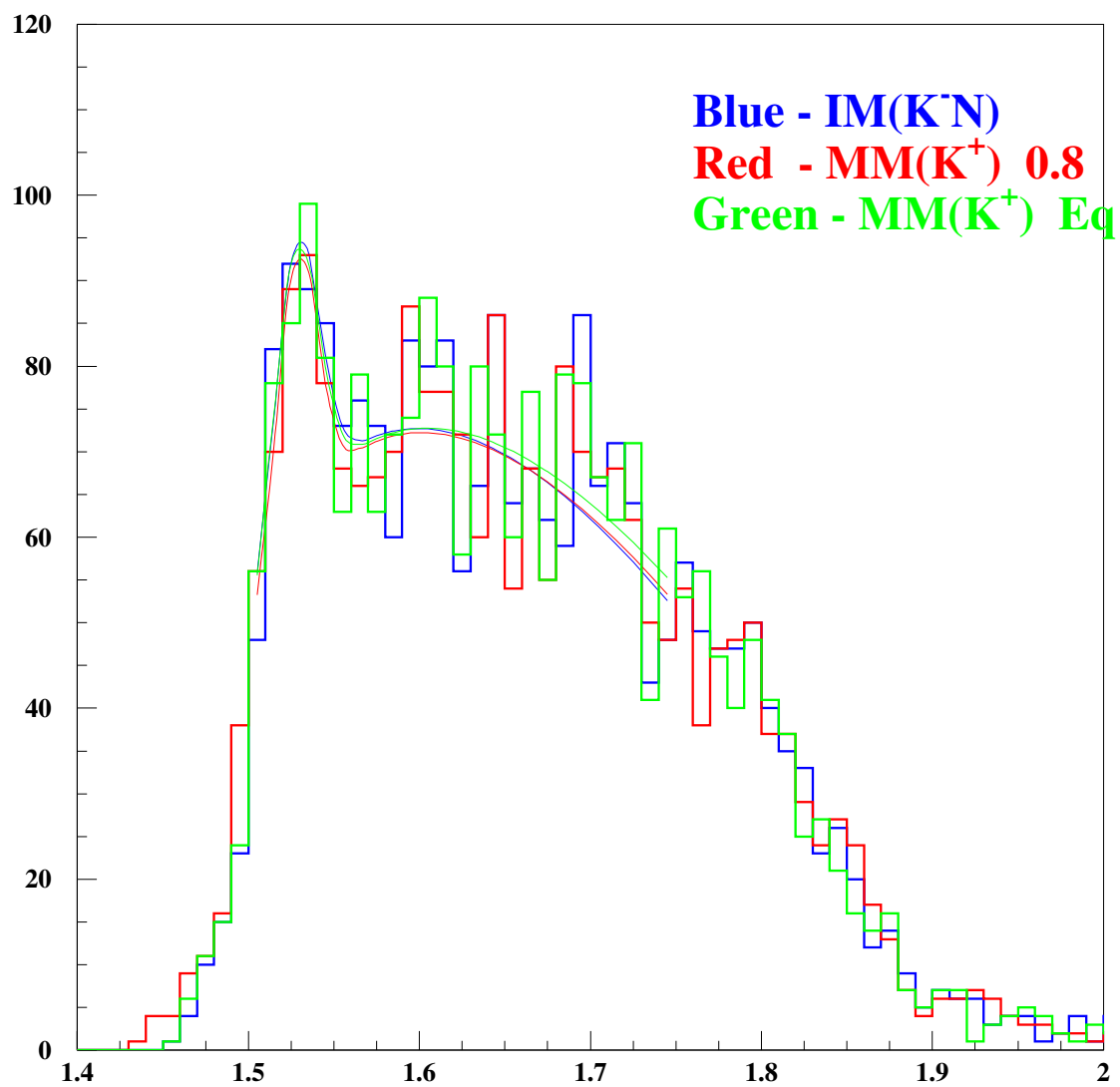


Figure 6: Comparison of the reconstructed $\Lambda^*(1520)$ by various methods. The distributions were created using the exact same event sample. The legends are the same as in the previous figure.